HHS Public Access

Author manuscript

Abdom Radiol (NY). Author manuscript; available in PMC 2019 April 13.

Published in final edited form as:

Abdom Radiol (NY). 2016 May ; 41(5): 844–853. doi:10.1007/s00261-015-0589-3.

DCE MRI of prostate cancer

Rose M. Berman[#1], **Anna M. Brown**[#1,2], **Silvia D. Chang**[3], **Sandeep Sankineni**[1], **Meet Kadakia**[4], **Bradford J. Wood**[5], **Peter A. Pinto**[4], **Peter L. Choyke**[1], and **Baris Turkbey**[1]

[1]Molecular Imaging Program, National Cancer Institute, National Institutes of Health, 10 Center Dr, MSC 1182 Bldg 10, Room B3B85, Bethesda, MD 20892-1088, USA

[2]Duke University School of Medicine, Durham, NC, USA

[3]Department of Radiology, University of British Columbia, Vancouver, BC, Canada

[4]Urologic Oncology Branch, National Cancer Institute, National Institutes of Health, Bethesda, MD, USA

[5]Diagnostic Radiology Department, Warren Grant Magnuson Clinical Center, National Institutes of Health, Bethesda, MD, USA

[#] These authors contributed equally to this work.

Abstract

DCE MRI is an established component of multi-parametric MRI of the prostate. The sequence highlights the vascularization of cancerous lesions, allowing readers to corroborate suspicious findings on T2W and DW MRI and to note subtle lesions not visible on the other sequences. In this article, we review the technical aspects, methods of evaluation, limitations, and future perspectives of DCE MRI.

Keywords

DCE MRI; Prostate cancer; Multi-parametric MRI

Prostate cancer (PCa) is the second most common cancer in men throughout the world, and the second highest cause of cancer-related deaths in the US [1]. In fact, on postmortem biopsies, pathologists note PCa in about 80% of both white and black American men in their 70's [2]. With widespread screening using serum prostate-specific antigen (PSA), standard biopsy rates and consequently PCa detection rates have shot up in the past few decades. However, a man's lifetime risk of developing PCa and dying of PCa is 16% and 2.9%, respectively [3], demonstrating that most disease diagnosed in men is indolent. This data suggests the need to reduce the unnecessary detection of low-risk disease and prolonged surveillance of patients with such disease.

Correspondence to: Baris Turkbey; turkbeyi@mail.nih.gov.

Electronic supplementary material The online version of this article (doi:10.1007/s00261-015-0589-3) contains supplementary material, which is available to authorized users.

Multi-parametric magnetic resonance imaging (mpMRI) has emerged as an excellent modality for ruling out high-risk PCa lesions, and can act along with PSA as an adjunct test for biopsy-naïve and biopsy-negative patients [4]. Furthermore, mpMRI can be used to assess patients for active surveillance (AS), monitor the risk category of patients already on AS [5], and select patients for MRI/TRUS fusion biopsy by detecting large and high-grade lesions [6]. Multi-parametric MRI includes anatomical sequences (T1- and T2-weighted MR imaging) and functional sequences (diffusion weighted MR imaging (DWI), dynamic contrast-enhanced MRI (DCE MRI), and more rarely MRI spectroscopy imaging (MRSI).

T1W MRI is mainly used within the framework of mpMRI to rule out post-biopsy hemorrhage in the prostate and to survey the entire pelvis for enlarged pelvic lymph nodes and possible bone metastases [7]. T2W MRI shows detailed zonal anatomy of the prostate and serves to not only detect lesions but also to evaluate extracapsular extension and seminal vesicle invasion [8], while DWI is an indicator of cellularity and tumor aggressiveness [9]. Lastly, DCE MRI assists in the interpretation of T2W MRI and DWI in detection of high-risk prostate cancer and surveillance status post-prostatectomy, -radiotherapy or -focal ablation [10, 11]. It primarily differentiates the tumor vasculature from the routine blood vessel network within the prostate through measuring vascular permeability and perfusion [12].

Like most other solid tumors, PCa exhibits tumor angiogenesis [13]. Vascular endothelial growth factor (VEGF) is associated with more angiogenesis and poorer outcomes [14, 15]. The new tumor vessels created during angiogenesis are thin, highly permeable, and irregular in shape, structure, and organization. Larger vessel diameter and irregular vascular morphology are vascular signs associated with an increased metastatic potential [16], and higher microvessel density is associated both with metastases and higher Gleason scores except for tumors located in the transition zone [17]. Moreover, the number of abnormal vessels observed in a tumor also inversely correlates with the prognosis [17, 18]. Considering the major role of VEGF and angiogenesis in the spread of PCa, DCE MRI is a natural tool for evaluating the presence of tumor angiogenesis as a distinguishing imaging sign of malignancy. This paper will discuss the strengths and limitations of DCE MRI for detecting prostate cancer within the framework of mpMRI.

What is DCE MRI?

DCE MRI produces a minimally invasive visualization of tumor angiogenesis. The sequence comprises T1-weighted (T1W) fast gradient echo images of the prostate obtained before, during, and after intravenous injection of a low molecular-weight gadolinium chelate. Because of the disorganization and increased permeability of the tumor vessels [19], the gadolinium contrast washes in and out of the tumor more rapidly than in normal tissue. Cancerous lesions therefore appear hyper-intense, at least initially, on DCE MRI (Figs. 1, 2, 3).

Technical aspects of DCE imaging

The recently released American College of Radiology (ACR) Prostate Imaging Reporting and Data System (PIRADS) v2 aims to standardize the acquisition of the DCE MRI sequence, which had been highly variable and inconsistently acquired in the past (Table 1). The major parameters of a DCE MRI acquisition, temporal resolution and total acquisition duration, vary greatly across centers. PIRADS v2 recommends a temporal resolution of ≤15 s (though many centers prefer under 7 s) and total acquisition duration of ≥2 min [23]. In addition, practitioners should adjust spatial resolution in order to avoid volume averaging and allow for the optimum imaging of suspicious lesions. With the use of the minimum requirement parameters, it is hoped that there will be more consensus on the use of DCE MRI in prostate cancer imaging and management.

One of the important questions for DCE MRI is whether to use a 1.5T or 3T magnet system. In general, 3 Tesla provides higher signal-to-noise ratio (SNR) than 1.5 Tesla MRI. The higher SNR strength enables a decrease in acquisition time resulting in increased temporal resolution. The higher SNR can also be used to improve spatial resolution. There are few studies directly comparing DCE at 1.5 Tesla and 3 Tesla [20]. Sertdemir et al. suggested improved performance at 3 T. For instance, it was shown that the ability to differentiate prostate cancer from normal tissue and prostatitis is improved at 3 Tesla [21].

While data are limited, it is widely understood that image quality is improved with the use of the endorectal coil (ERC), and specifically at 3 Tesla. However, the decision to use an ERC is controversial as there are added costs and discomfort associated with doing so. Thus, there remains an ongoing debate as to whether the ERC improves sensitivity, specificity and/or overall accuracy. Few large institutions still perform mpMRI with ERC due to the additional time and expense. However, it seems that there may be a justified role for ERC in post-therapy follow-up imaging to detect local recurrence. After focal therapy and/or prostatectomy, the higher SNR provided by the ERC improves the image quality and thus the sensitivity for residual and/or recurrent disease, which is often quite subtle [22]. At this time, larger studies are still required to solidify the use of ERC with mpMRI in cancer detection, active surveillance, treatment follow-up and for monitoring of disease recurrence.

Evaluation and interpretation of DCE MRI of the prostate

There are three methods for analyzing DCE MRI: qualitative, semi-quantitative, and quantitative. Although there are published studies on all three of these techniques, there is very limited data comparing these techniques to each other. Each method has its own advantages and limitations. Currently, there is no consensus on the standardization of DCE MRI although PIRADS version 2 [23] favors the qualitative method.

Qualitative analysis is the most common method owing to its ease of use and availability, as it does not require additional software or hardware. This technique consists of a visual assessment of focal areas that enhance early and more intensely than normal tissue (Fig. 4). Cancers also tend to washout of contrast faster than normal tissue and benign hyperplasia [11, 24, 25]. These features reflect angiogenesis of the tumor as flow is increased, resistance

is decreased and increased interstitial pressures force the contrast back into the vessels accounting for washout [17, 26–28]. The visual method of assessment is used in PIRADS version 2, as it does not require specific software [23]. A lesion is considered positive on DCE MRI when it exhibits focal enhancement earlier or contemporaneously with normal prostatic tissue, and when there are corresponding findings on T2W and/or DWI. Alternatively, DCE MRI is negative in the absence of early enhancement of the contrast media, or in the presence of diffuse enhancement that does not correspond with a focal finding on T2W and/or DW MRI. There is, however, overlap between benign and malignant tissues in both the peripheral and the transition zones; some benign lesions such as benign prostatic hyperplasia (BPH) nodules show strong early enhancement, while some malignant lesions do not show early enhancement or washout [29, 30]. Although qualitative analysis is the easiest of the three techniques to implement, it is the most subjective and the least standardized.

Semi-quantitative analysis is also based on the premise that tumors demonstrate more rapid and more intense early enhancement. This method involves placing an electronic region of interest (ROI) and tracking the time-intensity curves. While the overall shape of the curve is the most important feature, other parameters include the time of first contrast uptake, time to peak, maximum slope, and peak enhancement [31, 32]. There are three types of dynamic contrast enhancement curves: type 1 demonstrates progressive enhancement, type 2 demonstrates rapid enhancement and then plateaus, and type 3 demonstrates rapid enhancement and then washout. These dynamic curve types were used in the original PIRADS version 1 scoring system [33]. Because prostate cancer has been shown to demonstrate early intense enhancement with rapid washout of contrast [1], the type 3 curve is considered the most suspicious for prostate cancer. However, prostate cancers can also exhibit type 1 and type 2 curves and thus ‘‘curve shape’’ is not specific [30]. There are commercial products that display qualitative parameters such as those described above in a color-coded format.

The use of dynamic curves is a relatively simple approach that can help differentiate malignant from normal tissue [31], but the method has many limitations. One must keep in mind that the qualitative nature of curve typing is dependent on the quality of the injection and it provides no physiologic insight into the underlying pathology. It can therefore be difficult to compare the results obtained at different institutions. The PIRADS Steering Committee has concluded that there is not enough peer-reviewed published data or expert consensus to support the clinical use of semi-quantitative methods in DCE MRI analysis [23].

Quantitative analysis is the most complex of the methods used to analyze DCE MRI, requiring additional software. The two-compartment pharmacokinetic Tofts model is most commonly used [34]. This method does not rely on signal intensity but rather on the calculated concentration of gadolinium in the tumor, enabling quantification of contrast agent exchange between the intravascular and the extravascular extracellular space. The Tofts model fits various parameters to the time gadolinium concentration curve generated during DCE MRI. It incorporates an arterial input function to calculate the constants K^{trans}, k_{ep}, and v_e. $K^{trans}$is the volume transfer constant between blood plasma and the

extravascular extra-cellular space of the tumor. This is a measure of the permeability of the vasculature, also known as the rate of influx/wash-in. v_e is the fractional volume of extravascular extracellular space, and the constant k_{ep} is the quotient derived from dividing K^{trans} by v_e, representing the efflux/washout from the extravascular extracellular space back to plasma. Both K^{trans} and k_{ep} have been shown to be elevated in cancers [35, 37], and commercial software programs are available to produce color-encoded K^{trans} and k_{ep} maps. This quantitative method is the most objective, as it is not influenced by technical variations such as injection rates. However, there is also overlap of the rate constants for benign and malignant tissue. This type of analysis is also the most complex and most time intensive method of assessing DCE MRI, and the current expert opinion is that there is inadequate published data to support its widespread clinical use.

Studies have examined all three techniques, with varying results [24, 29–40]. Hansford et al evaluated the performance and inter-observer agreement of qualitative DCE MRI curve analysis for the differentiation of prostate cancer from healthy prostatic tissue in the PZ in 120 patients. They reported similar ROC curves for all observers, but mean areas under the receiver operating characteristic curve were poor (0.58 ± 0.04 [standard deviation] to 0.63 ± 0.04) [30]. Ocak et al. evaluated quantitative approach in 50 patients and reported overall sensitivity, specificity, PPV, and NPV of T2-weighted imaging as 94%, 37%, 50%, and 89%, respectively. The sensitivity, specificity, PPV, and NPV of dynamic contrast-enhanced MRI were 73%, 88%, 75%, and 75%, respectively, in that cohort. Additionally, the K^{trans}, k_{ep}, and AUC were significantly higher ($p < 0.001$) in cancer than in the normal peripheral zone [38].

It is clear that the evaluation and interpretation of DCE MRI is complex, with multiple factors at play. Therefore, DCE MRI should always be read in conjunction with the other MRI sequences. In addition, the variability in technique and interpretation makes standardization difficult to implement across all institutions—the optimal technique still needs to be established.

Current use of DCE MRI in prostate cancer

Cancer detection in treatment-naïve patients

The use of DCE MRI, once a mainstay of prostate MRI, is now much more controversial. In a study of 70 patients who later underwent radical prostatectomy, Turkbey et al. found that DCE MRI and T2W MRI resulted in a probability of tumor detection of 0.58, compared to 0.40 when T2W MRI was used alone [41]. Though DCE MRI cannot be used alone to identify tumors, the sequence's high-contrast images and improved spatial resolution over DWI can aid readers in increasing the PIRADS score of lesions equivocal on DWI imaging (Fig. 2) [23]. DCE MRI is especially valuable for evaluating lesions in regions of the prostate that are challenging to evaluate, such as the central zone, distal apex, anterior fibromuscular stroma, and subcapsular regions [42]. In these cases, a reader may see a subtle lesion on other sequences and turn to DCE MRI to further evaluate and/or confirm suspicion.

On the other hand, a recent meta-analysis of 22 studies aimed at evaluating the role of DCE MRI in detecting PCa found that, although DCE MRI improved tumor detection when compared to T2W alone (0.82–versus 0.68–0.77). Moreover, the partial AUC for the combination of DCE MRI, DWI, and T2W MRI was improved significantly (0.111; 0.103–0.119) when compared with DCE MRI alone (0.079; 0.072–0.085) and T2W MRI alone (0.079; 0.074–0.084) but not DWI alone (0.099; 0.091–0.108) [43]. Though it is clear that DCE MRI assists readers in identifying abnormalities in specific cases during an mpMRI examination, more extensive studies will be necessary to clarify the exact additive role of the sequence.

Cancer detection in post-treatment patients

DCE MRI is the most important mpMRI sequence for assessing for local recurrence of prostate cancer or residual disease, given the altered anatomy following definitive therapy [44].

Compared to T2W MRI alone, several studies have shown that the combination of T2W MRI with either DCE MRI or DWI performs better for detecting local recurrent prostate cancer after radical prostatectomy at 3T. Cha et al. identified increased AUC values of 0.935 and 0.845 in two readers for the combination of T2W MRI and DCE MRI for evaluating suspected soft tissue lesions in the prostatectomy fossa compared to AUC values of 0.773 and 0.756 for the two readers using T2W MRI alone, respectively. This represented a significant improvement, with p values of <0.001 and 0.018 for the two readers, respectively [45]. Roy et al. found that the combined sensitivity for detecting locally recurrent prostate cancer was 100% for T2W MRI combined with DCE MRI compared to only 57% for T2W MRI alone [46]. DWI, which is so successful in patients before surgery, tends to be highly distorted due to surgical clips and other artifacts after surgery and thus has less utility in the post-operative patient. Two other studies showed similar findings for detecting local recurrence using DCE MRI at 1.5T [47, 48]. These studies indicate that there is added value to using DCE MRI together with T2W MRI for detecting recurrent prostate cancer (Fig. 5).

DCE MRI has also been evaluated as a biomarker to assess response to focal therapy for recurrent prostate cancer. Barrett and colleagues investigated the accuracy of DCE MRI for predicting patient response to photo-dynamic therapy (PDT) applied as salvage treatment for prostate cancer patients who previously underwent definitive external beam radiation therapy (EBRT). They found that DCE MRI performed one week into PDT accurately predicted disease recurrence with 100% sensitivity, 60% specificity, 83% positive predictive value, and 100% negative predictive value, and thus showed promise for assessing patient outcome [49]. Though the population size was small (n = 15), the findings were encouraging and DCE MRI correlated better with patient outcome than prostate-specific antigen (PSA) levels, which decreased for 13/15 patients in the study.

Assessment of tumor aggressiveness

The aggressiveness of prostate cancer can be assessed in a number of ways, either based on the histologic grade defined by the Gleason score or, preferably, by response to therapy. However, the latter requires a considerable amount of time. Thus, predictive markers of

aggressiveness have clinical importance. In a cohort of 87 patients in which DCE MRI was performed prior to and after radiation therapy, Low et al. found that the K^{trans} values correlated with Gleason score, with the highest K^{trans} values corresponding to the highest Gleason score of 9, and these differences in K^{trans} persisted 2 months after treatment although in 75% of cases there were reductions in K^{trans} after therapy. These findings demonstrate that DCE MRI may indicate the relative aggressive potential of prostate cancers, since K^{trans} was highest for the higher grade tumors [50].

Another study by Vos et al. retrospectively examined the correlation between quantitative DCE MRI parameters and peripheral zone tumor aggressiveness (as defined by Gleason score on radical prostatectomy). They found that three parameters were particularly useful for discriminating low vs. intermediate or high-grade prostate cancer: the 75th percentile of wash-in, K^{trans}, and K_{ep} (for all three, $p = 0.02$ and area-under-the-curve (AUC) = 0.72) [51]. While these distinctions were statistically significant, they may lose value in individual cases as there are considerable overlaps between the categories. Moradi et al. found positive correlations between Gleason score and K^{trans}, v_e (interstitial space volume) and v_p (plasma volume) [52]. Turkbey et al. found that lesions were generally easier to detect as their Gleason score increased and that DCE MRI findings correlated with Gleason score, although again there were considerable overlaps [53]. These three studies show that DCE MRI becomes increasingly more useful with higher grade Gleason scores, though tissue confirmation is always necessary to confirm the presence of cancer as these findings can be non-specific and there exists considerable overlap among categories.

Prior biologic studies of prostate pathologies provide a potential explanation for the correlation of DCE MRI features with Gleason grade. Franiel and colleagues found that high-grade prostate cancer had the highest measurements of perfusion calculated in units of $mL/cm^3/min$ from post-processing parametric maps of the DCE MRI dataset [54]. Low-grade cancer had lower average perfusion, and the perfusion of prostate cancer overall was higher than for chronic prostatitis and normal tissue. The delay (in seconds) was lowest for high-grade cancer compared to normal tissue, chronic prostatitis, and low-grade cancer, potentially providing a basis for differences in pharmacokinetic properties observed for the different Gleason score categories.

Challenges and limitations of DCE MRI

There are several important challenges and limitations to DCE MRI. First, the sequence is sensitive to motion resulting from bulk patient movement (‘‘squirming or restlessness’’) [55], rectal peristalsis, and continuous bladder filling [11]. Because the study takes place over two to five or more minutes, there is ample opportunity for all types of motion, which leads to distortions, low-quality dynamic MR images and noisy curves [55] (Fig. 6 and Online Resource 1). Although it is not mandatory and may be difficult to perform, some papers have suggested that performing a rectal enema 1–3 h before MRI, using a glucagon-like anti-peristaltic agent, and recommending 4–6 h of fasting can decrease intestinal motion [55, 56]. Clinicians may be able to minimize discomfort from the ERC using a pelvic phased array coil instead, although Aydin et al. suggested that use of the latter decreases DCE MRI’s specificity, sensitivity, and positive and negative predictive values [55]. If motion

cannot be reduced during the study, commercially available DCE MRI post-processing software can attempt to realign the sequential images [11].

Another limitation of DCE MRI is its relative non-specificity. As discussed, tumors are not the only areas to show rapid enhancement and de-enhancement on DCE MRI—both prostatitis and highly vascularized BPH nodules can result in increased vessel enhancement [11]. Post-biopsy hemorrhages can also generate both false positive and false negative results. In addition, tumors in the anterior hypo-vascular transitional zone may not be apparent on DCE MRI because of their paucity of blood supply [11]. It is therefore necessary to interpret DCE MRI results in conjunction with the other mpMRI sequences.

Furthermore, DCE MRI adds cost compared to the other mpMRI sequences because it requires a bolus injection of gadolinium-based contrast media. Gadolinium chelates have a low risk of causing nephrogenic systemic fibrosis in patients with severe kidney failure, and those on dialysis are especially at risk. There is recent concern over the long-term deposition of gadolinium in parts of the brain and kidney. Exposure to intravenous gadolinium can lead to deposition of the contrast media in neural tissue, even in patients with normal renal function [57]. The deposition appears to be cumulative over a patient's lifetime and can be detected after as few as four lifetime doses of the contrast agent. Clinicians may therefore need to weigh the benefits and risks of adding gadolinium-based contrast media to the prostate MRI.

A final limitation of DCE MRI is the difficulty of reproducing results across centers. Although the recent PIRADS v2 maps out guidelines for image acquisition, processing, and interpretation of DCE MRI, there remain sources of variability (such as availability of 3T scanners). In summary, although there are several limitations to DCE MRI, the literature consistently recommends that it should be included as part of the mpMRI protocol as it can be used as an additional tool for characterization of indeterminate findings based on T2W and DWI alone.

Future perspectives

PIRADS v1 (2012), put forward by the European Society of Urogenital Radiology (ESUR), supported the use of semi-quantitative DCE MRI enhancement curves in the scoring system. Type 1 (progressive), type 2 (plateau), and type 3 (washout) curves were given progressively higher scores that contributed to the overall assessment. However, in a 2014 study evaluating semi-quantitative DCE MRI analysis, Hansford et al. demonstrated that the curve-type analysis performed poorly in differentiating prostate cancer tissue from healthy tissue in the peripheral zone [30]. They also found that although inter-observer agreement was high for Type 3 curves, it was lower for Type 1 and Type 2 curves. Moreover, it became clear that each lesion harbored a variety of curve types. The study therefore underlined a weakness in the first version of PIRADS: semi-quantitative analysis of DCE MRI was not reliable for detecting cancer, and it was less reproducible than desired.

Accordingly, the PIRADS v2 guidelines attribute a more limited role to DCE MRI. The new guidelines acknowledge that the value of DCE MRI is not well established, and thus its role

in determining PIRADS v2 Assessment Category is minor as compared to T2W and DW MRI. DCE MRI can be used to better interpret a moderate PIRADS score for a lesion; for example, when DWI shows a PIRADS 3 lesion in the peripheral zone, a positive finding on DCE MRI upgrades the score to PIRADS 4. On the other hand, DCE MRI is not included in the overall assessment when the lesion scores low (PIRADS 1 or 2) or high (PIRADS 4 or 5), and it does not upgrade a PIRADS 3 score in the transition zone [23].

The parameters for optimum DCE MRI acquisition have been controversial. For example, there has been some debate as to the best temporal resolution for the sequence; as discussed, PIRADS v2 recommends a temporal resolution of ≤15 s (with <7 s preferred) [23], with a total observation time of at least 2 min. According to the PIRADS Steering Committee, this temporal resolution and duration of DCE MRI provides the best visualization of focal early enhancement. Some studies have suggested that readers should focus only on early enhancement, because washout is less significant to diagnosis. For example, a 2013 study by Rosenkrantz et al. observed that requiring evidence of early contrast media washout in order to label a region suspicious for cancer decreases sensitivity for a peripheral zone tumor [40]. If further studies demonstrate that observing washout is unnecessary, the DCE MRI study's total observation time could potentially be decreased.

In terms of post-study processing, the development of computer-aided diagnosis (CAD) systems is a recent advance. CAD systems aim to improve observer performance, especially among non-experts. A typical CAD system will process mpMRI images and create a diagnostic result, such as a color prediction map of the prostate showing areas likely to be cancerous [60]. CAD has shown promise in several studies [58, 59] as an automated, reproducible method of detecting prostate cancer, though large multi-center studies will be necessary for a more thorough evaluation of the technology. Most CAD systems utilize DCE MRI in creating their maps, though one recent study by Kwak et al. demonstrated an effective CAD using only T2W and high b-value DWI MRI [61].

As CAD systems improve, the interpretation of DCE MRI and the other mpMRI sequences will improve as well—an accurate reading will depend less on the experience of the radiologist and will take less time. Furthermore, as the PIRADS v2 guidelines gain prevalence, interpretation of DCE MRI results (whether by a radiologist or by CAD) will become more standardized across centers. In the future, it will be important to integrate the PIRADS v2 standardization of mpMRI image acquisition and processing parameters into the clinical context.

Conclusion

Though the exact value of DCE MRI is controversial, the sequence plays an important role in detecting and localizing recurrent cancer in patients with biochemical recurrence, evaluating indeterminate lesions in the peripheral zone, and detecting subtle lesions in anatomically challenging regions. The PIRADS v2 has defined optimum parameters for DCE MRI acquisition, which will lead to greater standardization of the sequence in the coming years. Although DCE MRI is less integral to PIRADS evaluation than in the past, it is still an important part of the mpMRI-based prostate examination.

Supplementary Material

Refer to Web version on PubMed Central for supplementary material.

References

1. Humphrey PA (2014) Cancers of the male reproductive organs. In: Stewart BW, Wild CP (eds) World cancer report Lyon: World Health Organization
2. Delongchamps NB, Singh A, Haas GP (2006) The role of prevalence in the diagnosis of prostate cancer. Cancer Control 13(3):158–168 [PubMed: 16885911]
3. Ries LAG, Melbert D, Krapcho M, et al. (eds) (1975–2004) SEER cancer statistics review, National Cancer Institute, Bethesda, MD 2007 Available on http://seer.cancer.gov/csr/1975_2004/
4. Fütterer JJ, Briganti A, De Visschere P, et al. (2015) Can clinically significant prostate cancer be detected with multiparametric magnetic resonance imaging? A systematic review of the literature. Eur Urol 68(6):1045–1053 [PubMed: 25656808]
5. Guo R, Cai L, Fan Y, et al. (2015) Magnetic resonance imaging on disease reclassification among active surveillance candidates with low-risk prostate cancer: a diagnostic meta-analysis. Prostate Cancer Prostatic Dis doi:10.1038/PCan.2015.20
6. Hoeks CM, Barentsz JO, Hambrock T, et al. (2011) Prostate cancer: multiparametric MR imaging for detection, localization, and staging. Radiology 261:46–66 [PubMed: 21931141]
7. Qayyum A, Coakley FV, Lu Y, et al. (2004) Organ-confined prostate cancer: effect of prior transrectal biopsy on endorectal MRI and MR spectroscopic imaging. Am J Roentgenol 183(4): 1079–1083 [PubMed: 15385308]
8. Hedgire SS, Eberhardt SC, Borczuk R, McDermott S, Harisinghani MG (2014) Interpretation and reporting multiparametric prostate MRI: a primer for residents and novices. Abdom Imaging 39(5): 1036–1051 [PubMed: 24566965]
9. Alonzi R, Padhani AR, Allen C (2007) Dynamic contrast enhanced MRI in prostate cancer. Eur J Radiol 63:335–350 [PubMed: 17689907]
10. Tan CH, Wang J, Kundra V (2011) Diffusion weighted imaging in prostate cancer. Eur Radiol 21:593–603 [PubMed: 20936413]
11. Verma S, Turkbey B, Muradyan N, et al. (2012) Overview of dynamic contrast-enhanced MRI in prostate cancer diagnosis and management. Am J Roentgenol 198(6):1277–1288 [PubMed: 22623539]
12. Bonekamp D, Macura KJ (2008) Dynamic contrast-enhanced magnetic resonance imaging in the evaluation of the prostate. Top Magn Reson Imaging 19(6):273–284 [PubMed: 19512849]
13. Turkbey B, Mena E, Aras O, et al. (2013) Functional and molecular imaging: applications for diagnosis and staging of localised prostate cancer. Clin Oncol 25(8):451–460
14. Wegiel B, Bjartell A, Ekberg J, et al. (2005) A role for cyclin A1 in mediating the autocrine expression of vascular endothelial growth factor in prostate cancer. Oncogene 24:6385–6393 [PubMed: 16007189]
15. Green MM, Hiley CT, Shanks JH, et al. (2007) Expression of vascular endothelial growth factor (VEGF) in locally invasive prostate cancer is prognostic for radiotherapy outcome. Int J Radiat Oncol Biol Phys 67:84–90 [PubMed: 17189065]
16. Mucci LA, Powolny A, Giovannucci E, et al. (2009) Prospective study of prostate tumor angiogenesis and cancer-specific mortality in the health professionals follow-up study. J Clin Oncol 27:5627–5633 [PubMed: 19858401]
17. Erbersdobler A, Isbarn H, Dix K, et al. (2010) Prognostic value of microvessel density in prostate cancer: a tissue microarray study. World J Urol 28:687–692 [PubMed: 19714336]
18. Mucci LA, Powolny A, Giovannucci E, et al. (2009) Prospective study of prostate tumor angiogenesis and cancer-specific mortality in the Health Professionals Follow-Up Study. J Clin Oncol 27:5627–5633 [PubMed: 19858401]
19. Folkman J (1971) Tumor angiogenesis: therapeutic implications. N Engl J Med 285:1182–1186 [PubMed: 4938153]

20. de Bazelaire CM, Duhamel GD, Rofsky NM (2004) MR imaging relaxation times of abdominal and pelvic tissues measured in vivo at 3.0 T: preliminary results. Radiology 230(3):652–659 [PubMed: 14990831]
21. Sertdemir M, Schoenberg SO, Sourbron S (2013) Interscanner comparison of dynamic contrast-enhanced MRI in prostate cancer: 1.5 versus 3 T MRI. Invest Radiol 48(2):92–97 [PubMed: 23249646]
22. Muller BG, Kaushal A, Sankineni S, et al. (2015) Multiparametric magnetic resonance imaging-transrectal ultrasound fusion-assisted biopsy for the diagnosis of local recurrence after radical prostatectomy. Urol Oncol 33(10):425.e1–425.e6
23. American College of Radiology (2015) MR prostate imaging reporting and data system version 2.0 http://www.acr.org/Quality-Safety/Resources/PIRADS/. Accessed 7 2015
24. Engelbrecht MR, Huisman HJ, Laheij RJ, et al. (2003) Discrimination of prostate cancer form normal peripheral zone and central gland tissue by using dynamic contrast-enhanced MR imaging. Radiology 229:248–254 [PubMed: 12944607]
25. Girouin N, Mege-Lechevallier F, Tonina Senes A, et al. (2007) Prostate dynamic contrast-enhanced MRI with simple visual diagnostic criteria: is it reasonable? Eur Radiol 17(6):1498–1509 [PubMed: 17131126]
26. Nicholson B, Schaeffer G, Theodorescu D (2001) Angiogenesis in prostate cancer: biology and therapeutic opportunities. Cancer Metastasis Rev 20:297–319 [PubMed: 12085968]
27. Bigler SA, Deering RE, Brawer MK (1993) Comparison of microscopic vascularity in benign and malignant prostate tissue. Human Pathol 24:220–226 [PubMed: 8432518]
28. Siegal JA, Yu E, Brawer MK (1995) Topography of neovascularity in human prostate carcinoma. Cancer 75:2545–2551 [PubMed: 7537624]
29. Oto A, Kayhan A, Jiang Y, et al. (2010) Prostate cancer: differentiation of central gland cancer from benign prostatic hyperplasia by using diffusion-weighted and dynamic contrast-enhanced MR imaging. Radiology 257(3):715–723 [PubMed: 20843992]
30. Hansford BG, Peng Y, Jiang Y, et al. (2015) Dynamic contrast-enhanced MR imaging curve-type analysis: is it helpful in the differentiation of prostate cancer from healthy peripheral zone? Radiology 275(2):448–457 [PubMed: 25559231]
31. Noworoslski SM, Henry RG, Vigneron DB, et al. (2005) Dynamic contrast-enhanced MRI in normal and abnormal prostate tissues as defined by biopsy, MRI and 3D MRSI. Magn Reson Med 53:249–255 [PubMed: 15678552]
32. Bonekamp D, Jacobs MA, El-Khouli R, et al. (2011) Advancements in MR imaging of the prostate; from diagnosis to interventions. RadioGraphics 31(3):677–703 [PubMed: 21571651]
33. Barentz JO, Richenberg J, Clements R, et al. (2012) ESUR prostate MR guidelines 2012. Eur Radiol 22(4):746–757 [PubMed: 22322308]
34. Tofts PS, Brix G, Buckley DL, et al. (1999) Estimating kinetic parameters from dynamic contrast-enhanced T(1)-weighted MRI of a diffusible tracer: standardized quantities and symbols. J Magn Reson Imaging 10(3):2223–2232
35. Van Dorsten FA, van der Graaf M, Engelbrecht MR, et al. (2004) Combined quantitative dynamic contrast-enhanced MR imaging and (1)H MR spectroscopic imaging of human prostate cancer. J Magn Reson Imaging 20:279–287 [PubMed: 15269954]
36. Knopp MV, Giesel FL, Marecos H, et al. (2001) Dynamic contrast-enhanced magnetic resonance imaging in oncology. Top Magn Reson Imaging 12:301–308 [PubMed: 11687716]
37. Futteter JJ, Engelbrecht MR, Huisman HJ, et al. (2005) Staging prostate cancer with dynamic contrast-enhanced endorectal MR imaging prior to radical prostatectomy: experienced versus less experienced readers. Radiology 237:541–549 [PubMed: 16244263]
38. Ocak L, Bernardo M, Metzger G, et al. (2007) Dynamic contrast-enhanced MRI of prostate cancer a 3T: a study of pharmacokinetic parameters. AJR 189(849):W192–W201
39. Isebart S, DeKeyzer F, Haustermans K, et al. (2012) Evaluation of semi-quantitative dynamic contrast-enhanced MRI parameters for prostate cancer correlation to whole-mount histopathology. Eur J Radiol 81:e217–e222 [PubMed: 21349667]
40. Rosenkrantz AB, Sabach A, Babb JS, et al. (2013) Prostate Cancer comparison of dynamic contrast-enhanced MRI techniques for localization of peripheral zone tumor. AJR 3:W471–W478

41. Turkbey B, Pinto PA, Mani H, et al. (2010) Prostate cancer: value of multiparametric MR imaging at 3 T for detection—histopathologic correlation. Radiology 255:89–99 [PubMed: 20308447]
42. Hansford BG, Karademir I, Peng Y, et al. (2014) Dynamic contrast-enhanced MR imaging features of the normal central zone of the prostate. Acad Radiol 21(5):569–577 [PubMed: 24703469]
43. Tan CH, Hobbs BP, Wei W, Kundra V (2015) Dynamic contrast-enhanced MRI for the detection of prostate cancer: meta-analysis. Am J Roentgenol 204:W439–W448 [PubMed: 25794093]
44. Muller BG, van den Bos W, Brausi M, et al. (2015) Follow-up modalities in focal therapy for prostate cancer: results from a Delphi consensus project. World J. Urol Available on http://www.ncbi.nlm.nih.gov/pubmed/25559111. Accessed 6 Jan 2015
45. Cha D, Kim CK, Park SY, Park JJ, Park BK (2014) Evaluation of suspected soft tissue lesion in the prostate bed after radical prostatectomy using 3T multiparametric magnetic resonance imaging. Magn Reson Imaging 33(4):407–412 [PubMed: 25527395]
46. Roy C, Foudi F, Charton J, et al. (2013) Comparative sensitivities of functional MRI sequences in detection of local recurrence of prostate carcinoma after radical prostatectomy or external-beam radiotherapy. Am J Roentgenol 200(4):W361–W368 [PubMed: 23521479]
47. Sciarra A, Panebianco V, Salciccia S, et al. (2008) Role of dynamic contrast-enhanced magnetic resonance (MR) imaging and proton MR spectroscopic imaging in the detection of local recurrence after radical prostatectomy for prostate cancer. Eur Urol 54(3): 589–600 [PubMed: 18226441]
48. Cirillo S, Petracchini M, Scotti L, et al. (2009) Endorectal magnetic resonance imaging at 1.5 Tesla to assess local recurrence following radical prostatectomy using T2-weighted and contrast-enhanced imaging. Eur Radiol 19(3):761–769 [PubMed: 18825386]
49. Barrett T, Davidson S (2014) Enhanced MRI as a predictor of vascular-targeted photodynamic focal ablation therapy outcome in prostate cancer post-failed external beam radiation therapy. Can Urol 8:708–714
50. Low RN, Fuller DB, Muradyan N (2011) Dynamic gadolinium-enhanced perfusion MRI of prostate cancer: assessment of response to hypofractionated robotic stereotactic body radiation therapy. Am J Roentgenol 197(4):907–915 [PubMed: 21940578]
51. Vos EK, Litjens GJS, Kobus T, et al. (2013) Assessment of prostate cancer aggressiveness using dynamic contrast-enhanced magnetic resonance imaging at 3 T. Eur Urol 64(3):448–455 [PubMed: 23751135]
52. Moradi M, Salcudean SE, Chang SD, et al. (2012) Multiparametric MRI maps for detection and grading of dominant prostate tumors. J Magn Reson Imaging 35(6):1403–1413 [PubMed: 22267089]
53. Turkbey B, Pinto P, Mani H, et al. (2010) Prostate cancer: value of multiparametric MR imaging at 3 T for detection—histopathologifc correlation. Radiology 255(1):89–99 [PubMed: 20308447]
54. Franiel T, Lü demann L, Rudolph B, et al. (2008) Evaluation of normal prostate tissue, chronic prostatitis, and prostate cancer by quantitative perfusion analysis using a dynamic contrast-enhanced inversion-prepared. Investig Radiol 43(7):481–487 [PubMed: 18580330]
55. Aydin H, Hekimogl B, Tatar IG (2013) Limitations, disabilities, and pitfalls of dynamic contrast-enhanced MRI as a diagnostic modality in prostate cancer. Am J Roentgenol 200(3):W326 [PubMed: 23436880]
56. Lim C, Quon J, McInnes M, et al. (2015) Does a cleansing enema improve image quality of 3T surface coil multiparametric prostate MRI? J Magn Reson Imaging 42(3):689–697 [PubMed: 25556957]
57. McDonald RJ, McDonald JS, Kallmes DF, et al. (2015) Intracranial gadolinium deposition after contrast-enhanced MR imaging. Radiology 275(3):772–782 [PubMed: 25742194]
58. Niaf E, Lartizien C, Bratan F, et al. (2014) Prostate focal peripheral zone lesions: characterization at multiparametric MR imaging-influence of a computer-aided diagnosis system. Radiology 271(3):761–769 [PubMed: 24592959]
59. Scheenen TWJ, Rosenkrantz AB, Haider MA, Fütterer JJ (2015) Multiparametric magnetic resonance imaging in prostate cancer management: current status and future perspectives. Investig Radiol doi:10.1097/RLI.0000000000000163

60. Wang S, Burtt K, Turkbey B, Choyke P, Summers RM (2014) Computer aided-diagnosis of prostate cancer on multiparametric MRI: a technical review of current research. BioMed Res Int 2014:789561 [PubMed: 25525604]

61. Kwak JT, Xu S, Wood BJ, et al. (2015) Automated prostate cancer detection using T2-weighted and high-b-value diffusion-weighted magnetic resonance imaging. Med Phys 42(5):2368–2378 [PubMed: 25979032]

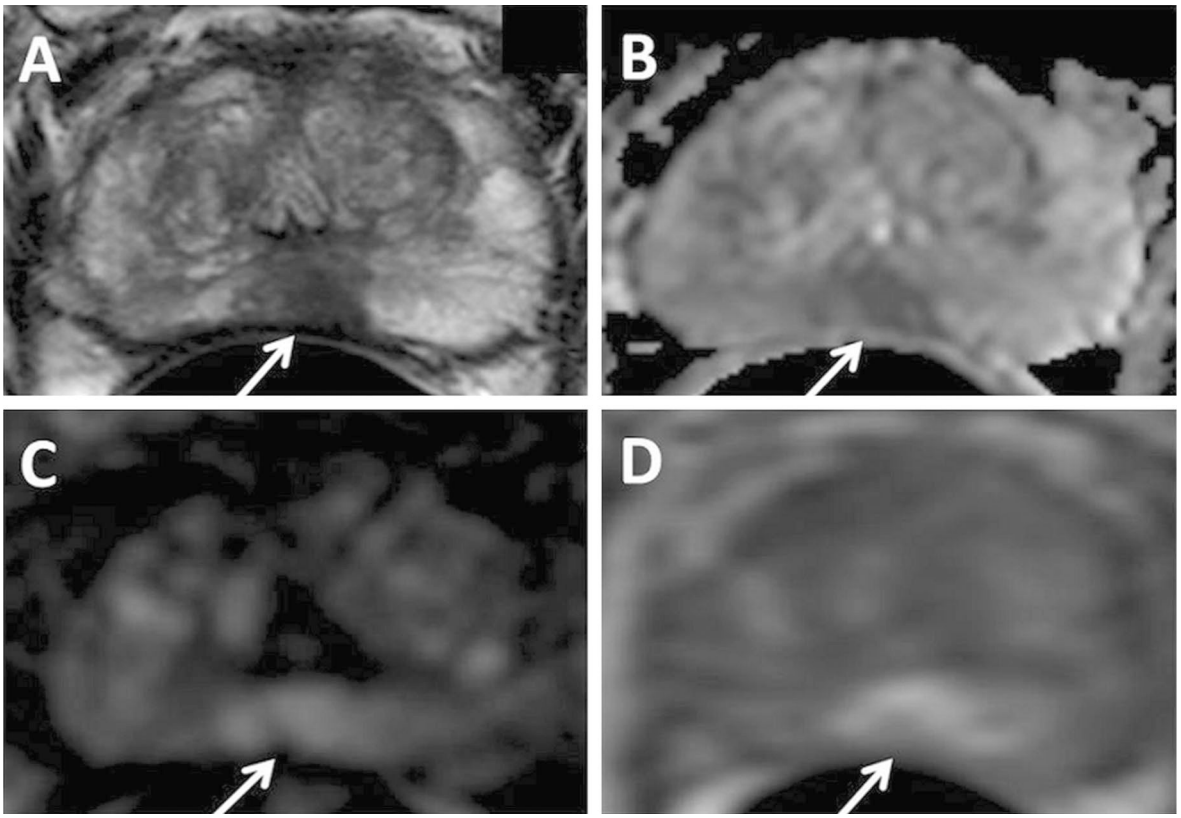

Fig. 1.

A 75-year-old man with PSA 10.23 ng/mL with no prior biopsy history. Axial T2W MRI (**A**) shows a hypointense lesion in the midline apical peripheral zone, which shows restricted diffusion on ADC map (**B**) and b2000 DW MRI (**C**) (*arrows*). The lesion shows positive enhancement on DCE MRI (**D**) (*arrow*). The lesion was found to have Gleason 8(4 + 4) prostate adenocarcinoma on targeted biopsy.

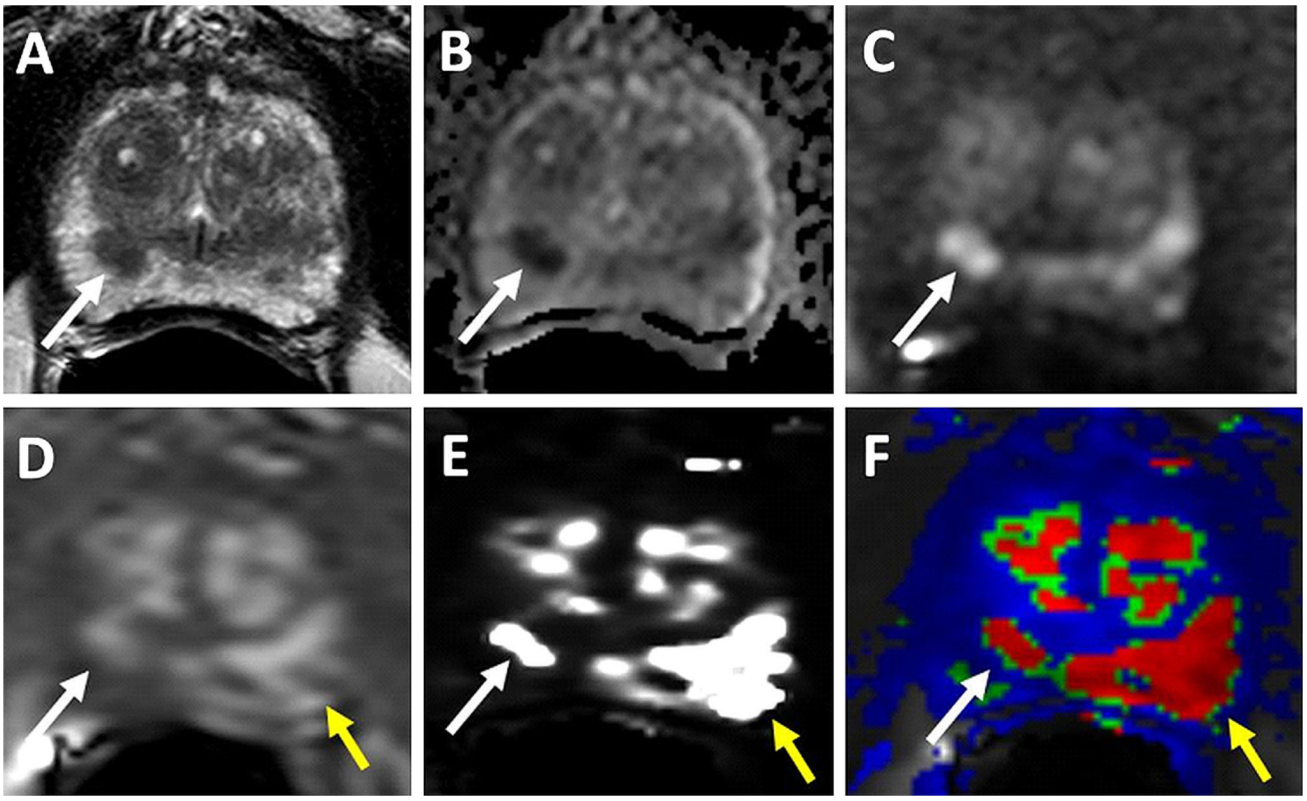

Fig. 2.

69-year-old man with PSA of 34.95 ng/mL. T2W (**A**), ADC map (**B**), b2000 DWI (**C**), raw DCE MRI (**D**) show a *right* mid peripheral zone lesion (Gleason 3 + 4 cancer at targeted biopsy). Raw DCE MRI (**D**), kep (**E**) and K^{trans} (**F**) mps show an additional lesion in the left mid peripheral zone (*yellow arrows*), which has subtle positive features on T2W MRI and DW MRI. This lesion includes Gleason 4 + 5 prostate cancer.

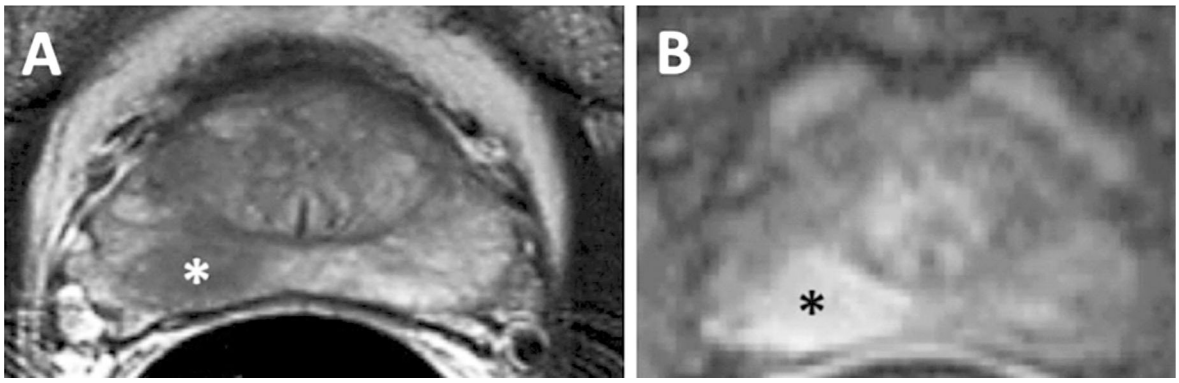

Fig. 3.

MRI with **A** T2 weighted and **B** DCE MRI in 67-year-old-man with a biopsy proven Gleason 3 + 4 in the right mid peripheral zone demonstrating an area of T2 hypointensity and an area of early enhancement (*asterisks*).

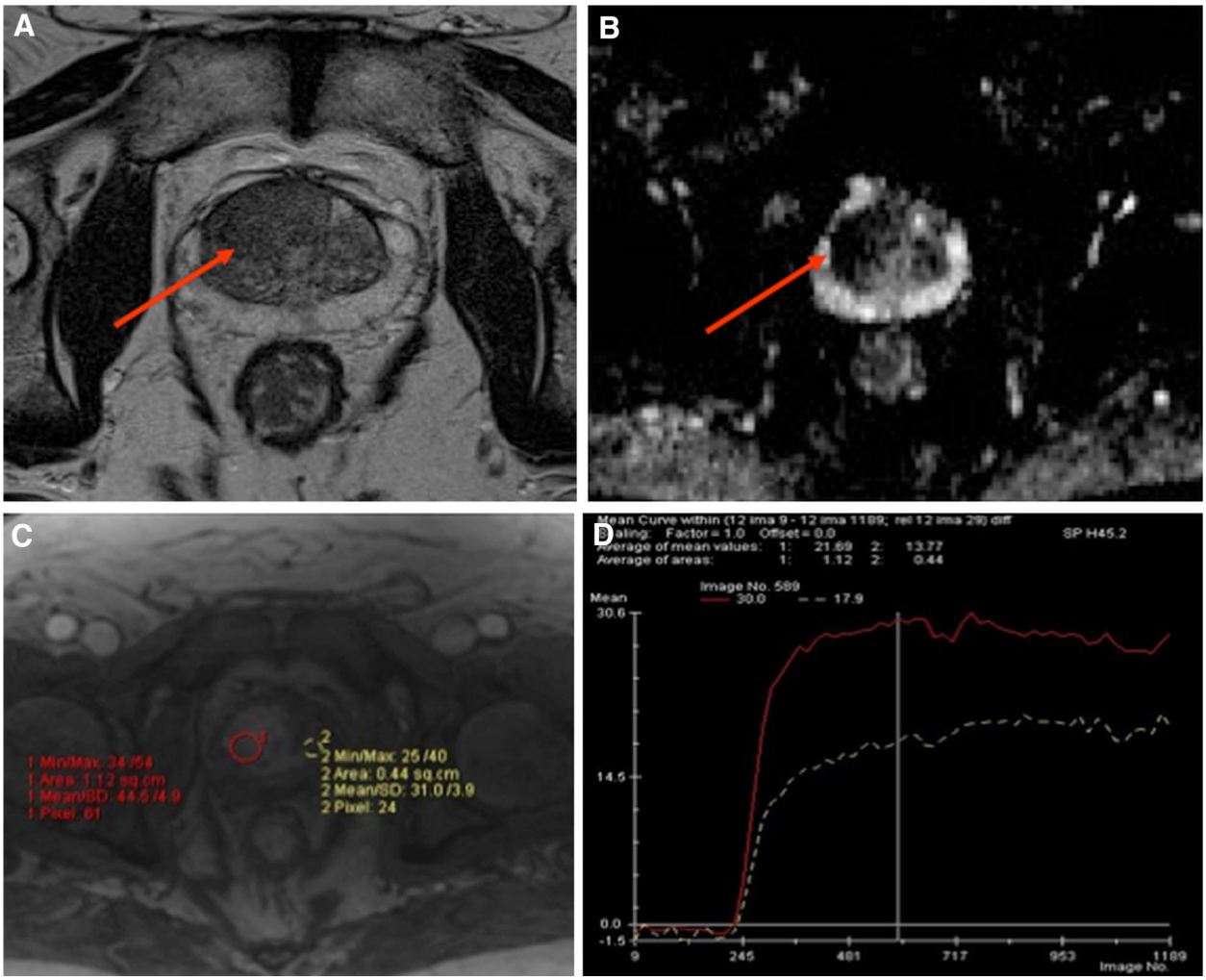

Fig. 4.

Multi-parametric MRI with **A** T2-weighted **B** ADC map **C** DCE and **D** time-intensity curve of the prostate on a 62-year-old man with a rising PSA of 10.8 and a previous negative prostate biopsy demonstrates a large area of low T2 signal intensity (*arrow*) with restricted diffusion with ADC of 877 (*arrow*) and hyperenhancement (*red circle*) demonstrating a Type 3 curve (*red curve*) compared normal tissue (*yellow circle*) demonstrating a Type 1 curve (*white curve*). Subsequent MRI-US fusion biopsy revealed Gleason 3 + 4.

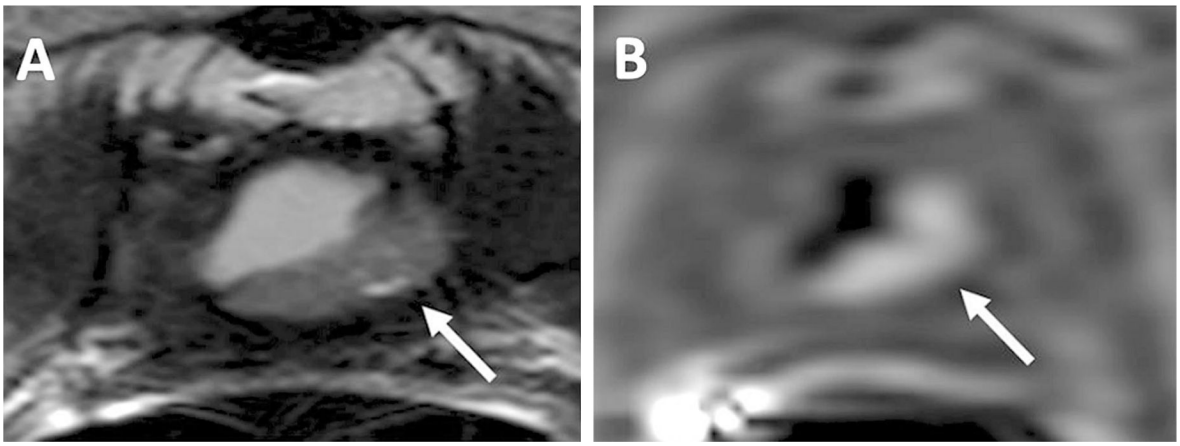

Fig. 5.

68-year-old man with a PSA = 11 ng/mL 6 years after prostatectomy. T2W MRI shows a lesion in the prostatectomy bed (*arrow*) **(A)**, DCE MRI shows hyperenhancement within the lesion confirming local recurrence (*arrow*) **(B)**.

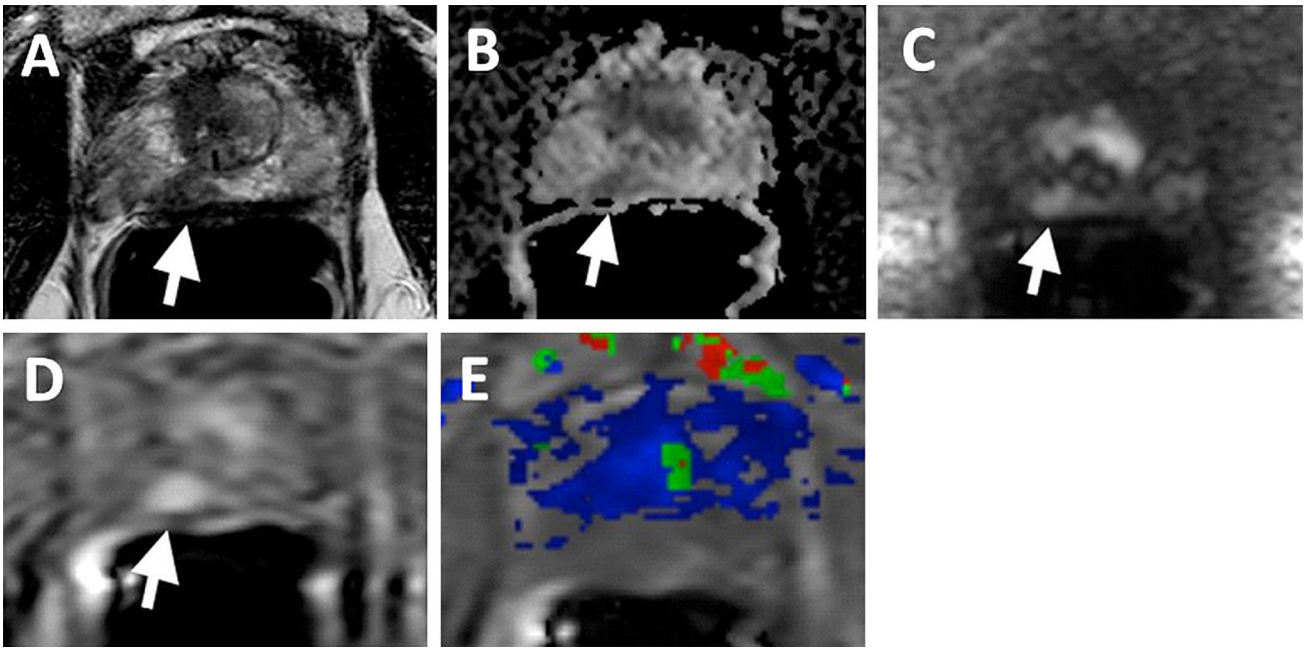

Fig. 6.

70-year-old man with a PSA of 5.67 ng/mL. T2W MRI **(A)**, ADC map **(B)**, b2000 DWI **(C)**, DCE MRI **(D)** shows a *right* mid peripheral zone lesion (arrows). K^{trans} map derived from DCE MRI **(E)** is obscured due to motion artifacts and lesion is not localized in the map (supplementary video).

Table 1.

PIRADS v2 recommended parameters for the DCE MRI sequence

DCE sequence parameters	2D or 3D T1 gradient echo (3D preferred)
TR/TE	<100 ms/<5 s
Slice thickness	3 mm, no gaps
Field of view	Entire prostate gland & seminal vesicles
In plane dimension	≤2 mm×≤2 mm
Temporal resolution	≤15 s (<7 s preferred)
Total observation time	≥2 min
Contrast dose	0.1 mmol/kg standard GBCA or equivalent high relaxivity GBCA
Contrast injection rate	2–3 cc/s with continuous image acquisition

Adapted from ACR PIRADS v2 [23]